EMBO reports

scientific report

Substrate binding to histone deacetylases as shown by the crystal structure of the HDAC8–substrate complex

Alessandro Vannini, Cinzia Volpari, Paola Gallinari, Philip Jones, Marco Mattu, Andrea Carfí, Raffaele De Francesco, Christian Steinkühler & Stefania Di Marco[+]

Istituto di Ricerche di Biologia Molecolare P. Angeletti, Pomezia, Rome, Italy

Histone deacetylases (HDACs)—an enzyme family that deacetylates histones and non-histone proteins—are implicated in human diseases such as cancer, and the first-generation of HDAC inhibitors are now in clinical trials. Here, we report the 2.0 Å resolution crystal structure of a catalytically inactive HDAC8 active-site mutant, Tyr306Phe, bound to an acetylated peptidic substrate. The structure clarifies the role of active-site residues in the deacetylation reaction and substrate recognition. Notably, the structure shows the unexpected role of a conserved residue at the active-site rim, Asp 101, in positioning the substrate by directly interacting with the peptidic backbone and imposing a constrained *cis*-conformation. A similar interaction is observed in a new hydroxamate inhibitor–HDAC8 structure that we also solved. The crucial role of Asp 101 in substrate and inhibitor recognition was confirmed by activity and binding assays of wild-type HDAC8 and Asp101Ala, Tyr306Phe and Asp101Ala/Tyr306Phe mutants.

Keywords: HDAC; acetylated substrate; mutagenesis; crystallography; drug design

EMBO reports (2007) **8**, 879–884. doi:10.1038/sj.embor.7401047

INTRODUCTION

Acetylation is a post-translational modification that controls the biological function and stability of proteins in eukaryotic cells. Unlike α-amino-terminal acetylation, ε-amino-lysine acetylation is reversible. Acetylation status of the lysine residue at the N-terminal extensions of core histones is controlled by two counteracting enzymes: histone acetyl transferases and histone deacetylases (HDACs; Roth *et al*, 2001; Marks *et al*, 2003). These activities affect histone–DNA interactions and their recognition by other chromatin-binding proteins. However, HDACs also participate in the regulation of non-histone proteins and are therefore important in many biological processes such as cell-cycle progression, cell survival and differentiation (Di Gennaro *et al*, 2004). As these processes are modulated during malignant transformation, HDAC inhibitors are being developed as anti-neoplastic drugs (Gallinari *et al*, 2007), and vorinostat was recently approved by the Food and Drug Administration for the treatment of cutaneous T-cell lymphoma.

Eukaryotic HDACs have been classified into four groups on the basis of phylogenetic analysis (Gregoretti *et al*, 2004). Class I HDACs include 1–3 and 8 (homologous to yeast Rpd3) and class II HDACs include 4–7, 9 and 10 (homologous to yeast Hda1), which are divided into two subclasses: IIa (4, 5, 7, 9) with one catalytic domain and IIb (6, 10) with two catalytic domains. HDAC11 is distinct from those in classes I and II; therefore, it has been placed in class IV, as class III refers to the unrelated sirtuin deacetylases (Blander & Guarente, 2004). HDACs 1–11 are metalloenzymes that require zinc for deacetylation; HDACs in classes I and IV are 350–500 residues in length, whereas class II HDACs are about 1,000 residues long. However, they all have homologous catalytic sites and are considered to go through a similar reaction mechanism (Holbert & Marmorstein, 2005).

With the exception of HDAC8, functional HDACs are not found as single polypeptides, but as high-molecular-weight multiprotein complexes (Yang & Seto, 2003), and most purified recombinant HDACs are enzymatically inactive (Sengupta & Seto, 2004). Therefore, from a structural biology perspective, HDAC8 is the best model among mammalian HDACs. Indeed, the crystal structure of HDAC8 in complex with inhibitors was recently solved and showed a compact α/β-domain composed of a central eight-stranded parallel β-sheet flanked by 11 α-helices (Somoza *et al*, 2004; Vannini *et al*, 2004), similar to the bacterial HDAC-like protein HDLP (Finnin *et al*, 1999) and the bacterial HDAC-like amidohydrolase HDAH (Nielsen *et al*, 2005). The HDAC8 active site (Somoza *et al*, 2004; Vannini *et al*, 2004) presents features of both serine and zinc proteases, and contains two His–Asp dyads with both histidine residues supposed to work as a general acid–base catalytic pair, as originally proposed for HDLP and extended to HDAH (Finnin *et al*, 1999; Nielsen *et al*, 2005). However, this mechanism has been questioned by theoretical studies, which indicate that the simultaneous protonation of both histidine residues is unlikely (Vanommeslaeghe *et al*, 2005).

Istituto di Ricerche di Biologia Molecolare P. Angeletti, Via Pontina Km 30.600, 00040 Pomezia, Rome, Italy
[+]Corresponding author. Tel: +39 0691093238; Fax +39 0691093654;
E-mail: stefania_dimarco@merck.com

Received 21 March 2007; revised 12 July 2007; accepted 12 July 2007; published online 10 August 2007

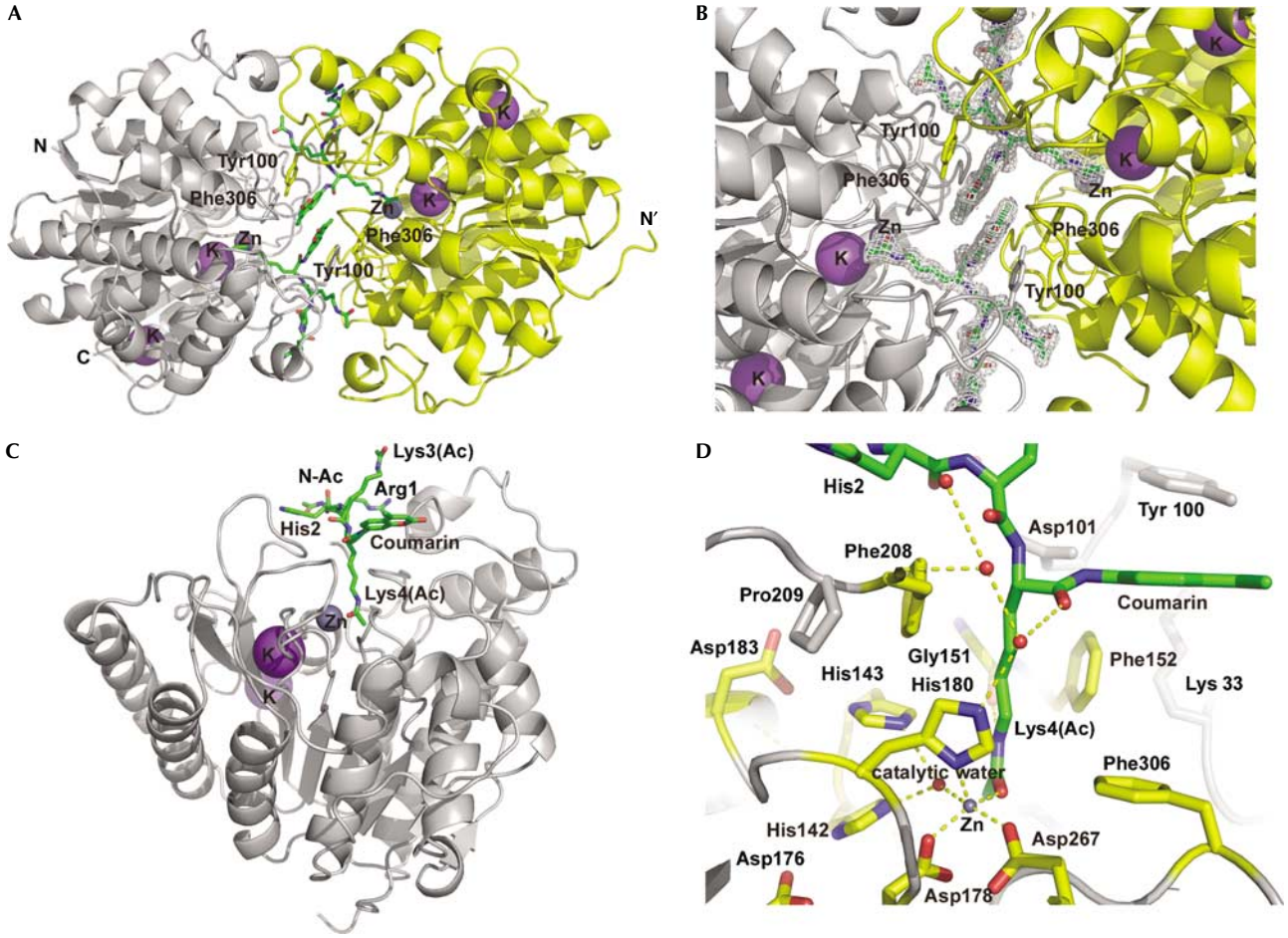

Fig 1 | Structure of the human HDAC8–substrate complex. (**A**) Ribbon diagram of the two HDAC8–substrate complexes in the asymmetric unit. The substrate and residues involved in the head-to-head packing are shown in a stick representation. Carbon, oxygen and nitrogen for the substrate are green, red and blue, respectively. Zn^{2+} and K^{+} ions are represented as purple spheres. (**B**) Enlarged view of the substrate-binding site in the asymmetric unit with the 1.0σ-contoured $2F_o-F_c$ electron density map. (**C**) HDAC8 monomer with the bound substrate. Atoms are coloured as in (**A**). (**D**) Enlarged view of the active site. Polar interactions are shown as dashed yellow lines. HDAC, histone deacetylase.

Moreover, a different type of mechanism with Tyr306, as a nucleophile, has been suggested (Kapustin *et al*, 2003).

To gain structural insights into acetylated substrate recognition and to clarify the deacetylation reaction, the structure of human HDAC8 in complex with a p53-derived diacetylated peptide, (acetyl)-L,Arg-L,His-L,Lys(ε-acetyl)-L,Lys(ε-acetyl), containing a fluorogenic coumarin group at its carboxyl terminus, was determined using X-ray crystallography at a resolution of 2.0 Å. In addition, we solved an HDAC8 structure in complex with a large hydroxamate inhibitor, (2*S*)-*N*8-hydroxy-2-{[(5-methoxy-2-methyl-1*H*-indol-3-yl)acetyl]amino}-*N*1-[2-(2-phenyl-1*H*-indol-3-yl) ethyl]octanediamide, at a resolution of 2.25 Å (supplementary Table S1 online).

RESULTS AND DISCUSSION

The substrate used for structural studies corresponds to the sequence Arg379-His380-Lys381(ε-acetyl)-Lys382(ε-acetyl) of the p53 tumour suppressor protein, localized in the C-terminal, basic regulatory domain of p53 (Liu *et al*, 1999). Lys382 deacetylation by class I HDACs results in repression of the transcriptional activity of p53 (Vaghefi & Neet, 2004). To trap the substrate in the crystal, we engineered a catalytically inactive HDAC8 mutant, Tyr306Phe (supplementary Fig S1 online). The overall structure of the complex shows a dimeric arrangement (Fig 1A,B), similar to HDAC8 structures with small hydroxamic acids, named compound 1 (Vannini *et al*, 2004) and Cra-19156 (Somoza *et al*, 2004). The main difference compared with these structures is the ordering of exposed loop regions, residues 84–105, following substrate binding, which produces a more compact protein conformation (supplementary Fig S2 online). The same dimeric arrangement and ordering of loop regions are observed in our new HDAC8–inhibitor structure (Fig 2; supplementary Table S1 online).

The structure of the monomer shows Lys382(ε-acetyl)—Lys4(Ac) of the substrate—protruding into the narrow cavity of the active site and coordinating Zn^{2+} through its carbonyl oxygen (Fig 1C). This lysine residue corresponds to the one deacetylated in p53 by class I HDACs (Vaghefi & Neet, 2004). In addition, there

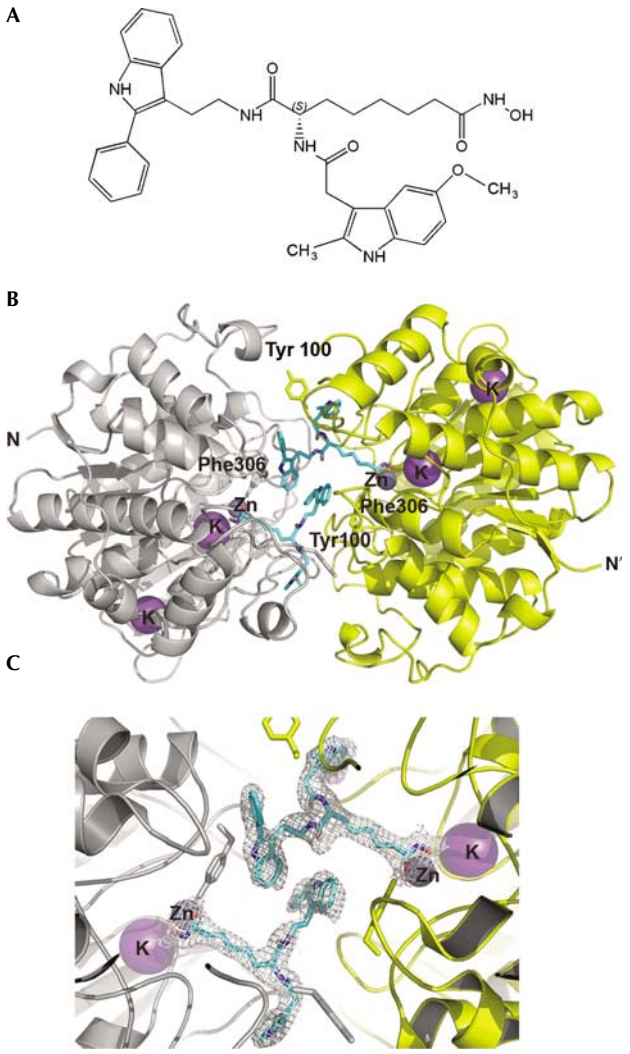

Fig 2 | Structure of the human HDAC8–inhibitor complex. (**A**) The hydroxamate inhibitor. (**B**) The two monomers in the asymmetric unit are in grey and yellow, respectively. The inhibitor and residues involved in the head-to-head packing are shown in a stick representation. Carbon, oxygen and nitrogen for the inhibitor are cyan, red and blue, respectively. (**C**) An enlarged view of the inhibitor-binding site in the asymmetric unit with 1.0σ-contoured $2F_o-F_c$ electron density map. HDAC, histone deacetylase.

is one water molecule that is Zn^{2+}-coordinated and interacts with His142 and His143, which is on the opposite side of the substrate with respect to residue 306 (Fig 1D). His142 is part of the buried and conserved charge–relay system, whereas His143 is part of the exposed putative charge–relay system, which is not conserved in HDACs (supplementary Fig S3 online). Therefore, Zn^{2+} is penta-coordinated with Asp178 (Oδ2, 1.97 Å), His180 (Nδ1, 2.07 Å) and Asp267 (Oδ2, 1.97 Å) as ligands, in addition to the water (2.07 Å) and the carbonyl oxygen (2.02 Å) of the acetyl group of the substrate (Fig 1D). The carbonyl carbon of the substrate is in close proximity to this active-site water molecule (2.34 Å) and also to the catalytic Zn^{2+} that polarizes the carbonyl group and orientates the water molecule, the nucleophilicity of which is increased further by hydrogen bonding to His142 and His143. The alkyl chain of Lys4(Ac) is also stabilized by hydrophobic interactions with Phe152 and Phe208, and one hydrogen bond to Gly151 (Fig 1D). In the structure of the HDAC8–inhibitor complex, the hydroxamate moiety establishes hydrogen bonds with His142, His143 and Tyr306, and coordinates Zn^{2+} in a bidentate fashion, with one of the oxygen atoms replacing the active-site water molecule (Fig 3A). The inhibitor-linker region fits in the hydrophobic channel and makes apolar interactions with Phe152 and Phe208, and van der Waals interactions with the main chain of Gly151 (Fig 3A). In HDACs there is a strict conservation of those residues contacting the Lys4(Ac) of the substrate or the hydroxamate–linker moieties of the inhibitor (supplementary Fig S3 online). The only significant exception is Tyr306, which is histidine in class IIa HDACs (4, 5, 7, 9), which causes a pronounced decrease in catalytic activity on peptidic substrates (Fischle *et al*, 2002).

Deacetylation should start with the nucleophilic attack by the active-site water molecule on the carbonyl carbon of the substrate (Fig 1D); His142 is suitably poised to abstract a proton from this water molecule. The interaction of the carbonyl oxygen of the substrate with Zn^{2+} results in enhanced polarization of the carbonyl bond, and hence is more susceptible to a nucleophilic attack. This mechanism is in agreement with what was previously proposed (Finnin *et al*, 1999; Somoza *et al*, 2004; Vannini *et al*, 2004; Nielsen *et al*, 2005), and excludes the role of residue 306 as a water-activated nucleophile (Kapustin *et al*, 2003; Vanommeslaeghe *et al*, 2003) because the active-site water molecule is far away from residue 306 and is on the opposite side with respect to the acetylated lysine (Figs 1D,3A). On nucleophilic attack—if we consider no rearrangement at the active site—His143 should be further away to protonate the amine-leaving group (Nε2—Nζ 3.79 Å), whereas Tyr306-hydroxyl group (Fig 3A) would be at a closer distance to donate a proton to the amine. The intermediate would then break, yielding acetate and lysine products. Here, by mutating Tyr306 to phenylalanine the substrate is bound but not hydrolysed, as the amino group of the intermediate is unable to be stabilized by binding to the tyrosine-hydroxyl, and is therefore trapped in the active site. Tyr306 is essential for activity on the peptidic substrate and also on purified histones (Fig 4A; supplementary Fig S1 online). Instead, the non-conservation of the exposed charge–relay system (His143/Asp183, Asn or Gln; supplementary Fig S3 online), the suggestion of recent theoretical studies of HDAC protonated at His142 but not at His143 (Vanommeslaeghe *et al*, 2005) and the finding that His143 mutation in HDAC1 reduced but did not abolish activity (Hassig *et al*, 1998) indicate a possible role of His143 in orientating the substrate rather than a role in protonating the amine-leaving group (Finnin *et al*, 1999; Somoza *et al*, 2004; Vannini *et al*, 2004; Nielsen *et al*, 2005).

An unexpected feature of this structure is at the rim of the active site, in which the side-chain carboxylate of Asp101 establishes two directional hydrogen bonds with two adjacent nitrogen atoms of the substrate backbone, constraining the latter in an unusual *cis*-conformation (Fig 3B). In addition, the two main-chain oxygen atoms of the substrate form a network of water-mediated hydrogen bonds with several protein residues (Fig 3B). Presumably, the tight polar interactions observed at the rim of the active site keep the

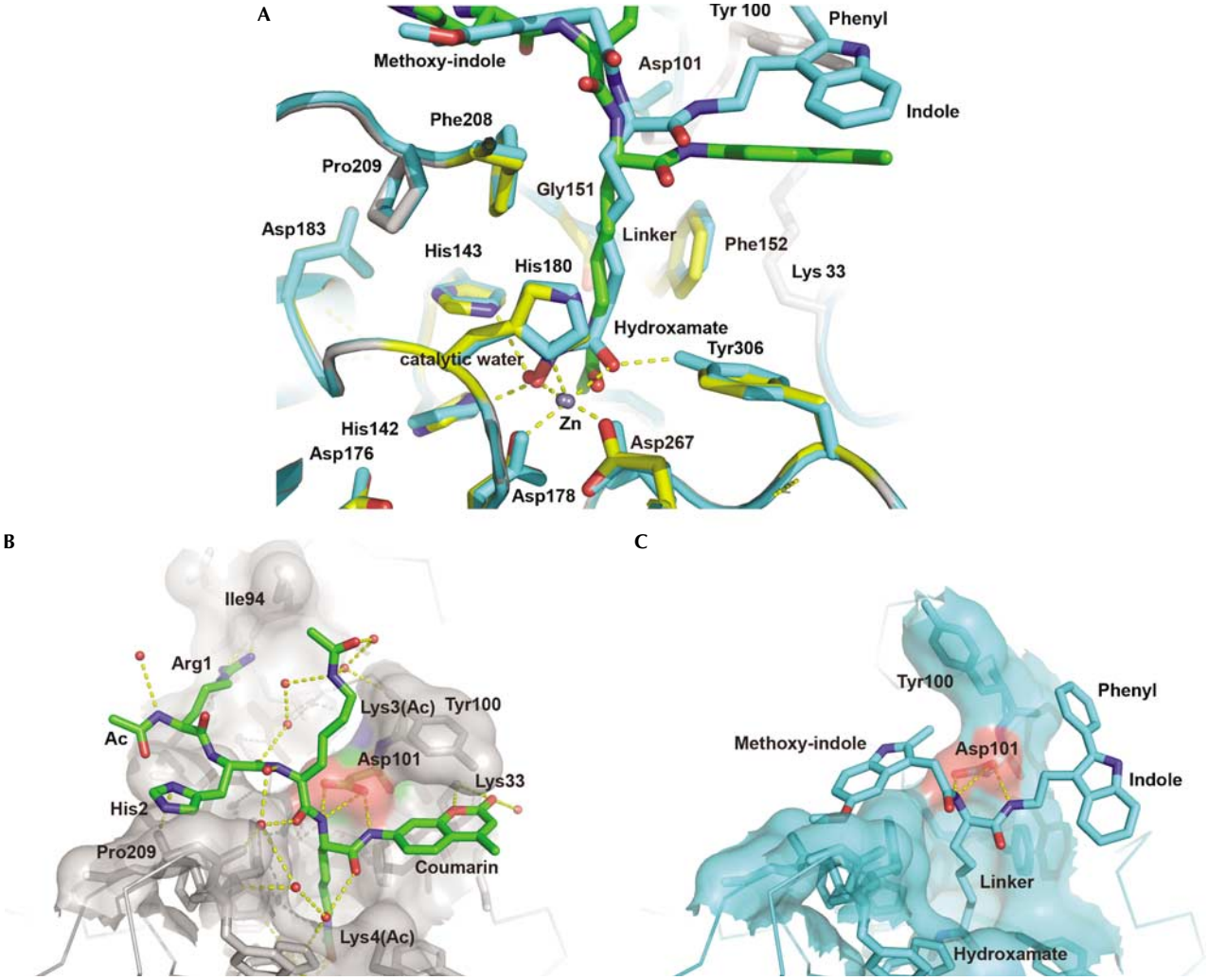

Fig 3 | Comparison of the structure of HDAC8–substrate with that of the HDAC8–hydroxamate inhibitor. (**A**) View of the substrate-binding site superimposed with the structure of the HDAC8–inhibitor (r.m.s.d.-Cα, 0.315 Å). Oxygen, nitrogen and carbon of the inhibitor are red, blue and cyan, respectively. Protein is cyan in the HDAC8–inhibitor structure. (**B**) Molecular surface of the HDAC8–substrate complex at the active-site entrance. Water molecules are shown as red spheres. (**C**) Molecular surface of the HDAC8–inhibitor complex. HDAC, histone deacetylase.

substrate in place during the deacetylation reaction. To confirm the relevance of this interaction, we mutated Asp101 to alanine. This mutation resulted in a complete loss of enzyme activity on the peptidic substrate and also on purified histones, despite the fold conservation (Fig 4A; supplementary Fig S1 online), indicating that this interaction is required for the correct positioning of substrates. In previous HDAC8 structures (Somoza *et al*, 2004; Vannini *et al*, 2004), the loop containing Asp101 (residues 98–105) is a region of high mobility with poor electron density. On substrate binding, this loop becomes structured (supplementary Fig S2 online, A compared with B and C). The importance of Asp101 in anchoring the substrate is not an exclusive feature of HDAC8, but might be extended to the whole family owing to the strict conservation of this residue in all class I and class II HDACs, despite the low overall sequence homology in this loop region and the presence of a long insertion in class IIa HDACs (supplementary Fig S3 online). Furthermore, it is important to note that, in the structure of the HDAC8–inhibitor complex, the same interaction with Asp101 is retained by the two inhibitor amide groups, despite the different conformer for the side chain of Tyr100 (Fig 3C). As a result of this interaction and differently from previous HDAC8-inhibited structures (supplementary Fig S2B,C online), in the structure reported here (Fig 2), these loop residues are all in density.

To validate further the role of Asp101, we carried out other biochemical experiments. In addition to the Asp101A mutant, we also produced the double mutant Asp101Ala/Tyr306Phe, which, as expected, was completely inactive (Fig 4A). Furthermore, the influence of the inhibitor and the peptidic substrate on the thermal stability of all mutants, and also on the wild-type protein, was evaluated by far-UV circular dichroism (CD) spectroscopy (supplementary information online). Only for wild-type HDAC8 did the thermal stability increase in the presence of the inhibitor ($\Delta T_m = 6.1\,^{\circ}C$; Fig 4B), whereas only for the Tyr306Phe mutant incubated with the peptidic substrate was there an increase in T_m

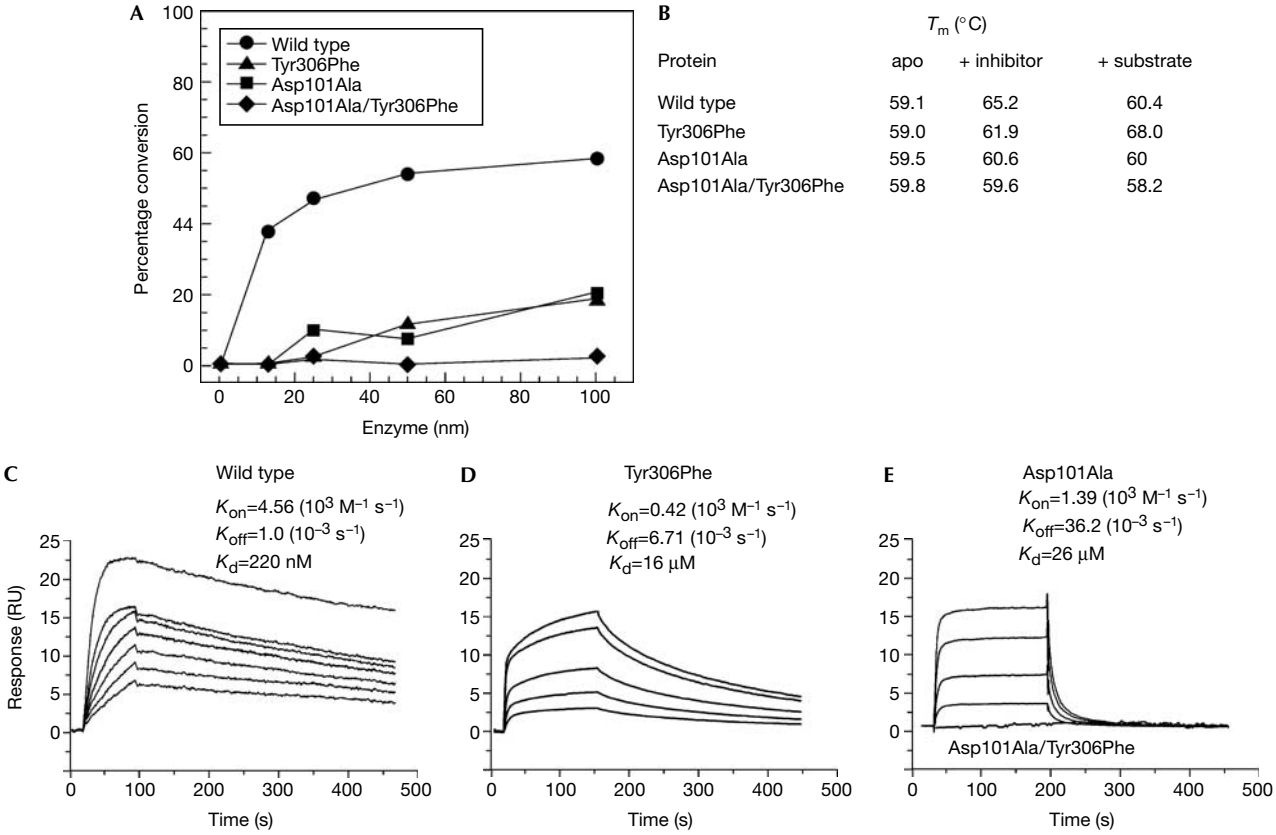

Fig 4 | Biochemical data supporting the Asp101 interaction hypothesis. (**A**) Deacetylase assay on purified histones of wild-type HDAC8 and mutants. (**B**) Thermally induced denaturation of wild-type HDAC8 and mutants by CD spectroscopy at 222 nm. The inhibitor is that used for crystallization, whereas the substrate has no coumarin group, substituted instead with Leu-Met and corresponding to p53 protein sequence 379–384 (Liu *et al*, 1999). (**C–E**) Surface plasmon resonance experiments of wild-type HDAC8 and mutants with the inhibitor. Protein concentration was 800 nM. Inhibitor concentrations going from top to bottom are (**C**) 10, 5, 2.25, 1.25, 0.625, 0.3 and 0.15 μM, (**D**) 100, 50, 25, 12.5 and 6.25 μM and (**E**) 100, 50, 25 and 12.5 μM. The last curve is the Asp101Ala/Tyr306Phe mutant with 100 μM inhibitor. CD spectroscopy, circular dichroism spectroscopy; HDAC, histone deacetylase.

($\Delta T_m = 9\,°C$; Fig 4B). These results confirm the relevance of Asp101 interactions (Fig 3B,C). We also carried out direct binding assays between all HDAC8 proteins and the inhibitor by surface plasmon resonance (SRP) experiments (Fig 4C–E; supplementary information online). These experiments were not possible with the substrate owing to the high K_m of the wild-type protein (67 μM), whereas the inhibitor had an HDAC8 IC_{50} of 100 nM (see supplementary information online). This IC_{50} is in line with the K_d measured by SRP (220 nM). The Tyr306Phe mutant had a strong decrease in the rate of complex formation (k_{on}) with the inhibitor, without much affecting the rate of dissociation (k_{off}; Fig 4D compared with C). The opposite was found for the Asp101Ala mutant that had a high k_{off}, but a k_{on} similar to that of the wild-type protein (Fig 4E compared with C), again indicating the importance of this residue for keeping the inhibitor in place. We did not observe a measurable binding with Asp101Ala/Tyr306Phe mutant (Fig 4E).

Furthermore, several of the most potent HDAC inhibitors—despite the large diversity in the cap moiety—have two amides as part of the cap (Jones *et al*, 2006; Rodriquez *et al*, 2006), and are therefore likely to establish such interactions with Asp101 in HDAC8 or corresponding aspartic acid residues in other HDACs. To this end, the importance of this interaction for drug-design purposes is shown by structure-activity relationship studies of HDAC1 inhibitors originating from a ketone variant (compound 1 in Jones *et al*, 2006 and in supplementary Table S2 online) of the hydroxamic acid compound presented here. Inversion of the stereocentre (compound 2), alkylation of either amides (compounds 3 and 4), homologation of the chains to β-amino acids (compounds 5 and 6) or main-chain shortening (compound 7) all destroy the activity of these compounds (supplementary Table S2 online). In summary, the substrate-bound and the inhibitor-bound structures presented here show the unexpected role of the conserved Asp101 residue not only for HDAC substrate recognition, but also as a hotspot for drug design of new antitumour agents.

METHODS

See the supplementary information online for protein production and activity assays, CD spectroscopy and thermal denaturation, and SRP.

Crystallization and diffraction data collection. HDAC8 point mutants Tyr306Phe and Ser39Asp, in 50 mM Tris–HCl (pH 8.0), 5% glycerol, 1 mM dithiothreitol and 150 mM KCl, were concentrated to 217 μM and 150 μM, respectively. Tyr306Phe-HDAC8 plus 3.2 mM substrate was crystallized at 22 °C by the hanging-drop method in 50 mM Tris–HCl (pH 8.0), 50 mM $MgCl_2$, 10% polyethylene glycol (PEG) 4000, 2 mM tri(2-carboxyethyl)phosphin (TCEP) and 30 mM glycyl-glycyl-glycine. Crystals were stabilized in 37.5 mM Tris–HCl (pH 8.0), 75 mM KCl, 25 mM $MgCl_2$, 10% glycerol, 20% PEG 4000, 1 mM TCEP and 50 μM substrate and then frozen in liquid nitrogen after gradually increasing PEG 4000 to 48%. For data collection, crystals were annealed for two cycles in a drop containing the same amount of cryoprotectant. Ser39Asp-HDAC8 plus 1.5 mM inhibitor was crystallized at 22 °C by the hanging-drop method in 50 mM 2-(*N*-morpholino)ethanesulphonic acid (MES, pH 6.8), 4% PEG 20000, 2 mM TCEP and 2% benzamidine. The Ser39Asp mutant is active and folded like wild-type protein (data not shown), and it was made for crystallization purposes because its crystals diffract better than wild-type protein. Crystals were stabilized in 25 mM Tris–HCl (pH 8.0), 25 mM MES (pH 6.8), 75 mM KCl, 15% glycerol, 8% PEG 20000, 1 mM TCEP and 100 μM inhibitor, before freezing them in liquid nitrogen by increasing PEG 20000 to 12%. Data were collected at 100 K using 0.931 Å wavelength synchrotron radiation at ESRF, Grenoble. Diffraction statistics are summarized in supplementary Table SI online.

Structure determination and analysis. Both structures were solved by molecular replacement with AMoRe (Navaza, 2001), using the Protein Data Bank entry 1w22 as a search model (Vannini *et al*, 2004). Dictionaries were generated with PRODRG (Schuttelkopf & van Aalten, 2004). Model building was carried out using QUANTA2000 (Accelrys, Cambridge, UK) and refinement with REFMAC (Murshudov *et al*, 1997). Final models encompass the following: for structure A (HDAC8–substrate)—one HDAC8 dimer in the asymmetric unit (AU) with each monomer consisting of residues 10–376 (A) or 15–377 (B), one substrate molecule, one Zn^{2+} and two K^+ ions, plus one glycyl-glycyl-glycine molecule in monomer B; for structure B (HDAC8 inhibitor)—one HDAC8 dimer in the AU and each monomer has residues 14–376, one inhibitor molecule, one Zn^{2+} and two K^+ ions. Both models show good stereochemistry, as assessed by PROCHECK (Laskowski, 2003), with 91% of total residues in the most favoured regions and 9% in additionally allowed regions of the Ramachandran plot, for structure A (90.5 and 9.5%, for structure B, respectively). Refinement statistics are listed in supplementary Table SI online. Figures were generated with PyMOL (DeLano Scientific).

Coordinates. The atomic coordinates and structure factors have been deposited with the Protein Data Bank (accession codes 2v5w and 2v5x).

Supplementary information is available at *EMBO reports* online (http://www.emboreports.org).

ACKNOWLEDGEMENTS

We thank the staff at beamline ID14-H3, European Synchrotron Radiation Facility (ESRF), Grenoble, for data collection assistance and C. Paolini for activity assay. This paper is dedicated to the memory of our beloved colleague Giovanni Migliaccio.

REFERENCES

Blander G, Guarente L (2004) The Sir2 family of protein deacetylases. *Annu Rev Biochem* **73:** 417–435

Di Gennaro E, Bruzzese F, Caraglia M, Abruzzese A, Budillon A (2004) Acetylation of proteins as novel target for antitumor therapy: review article. *Amino Acids* **26:** 435–441

Finnin MS, Donigian JR, Cohen A, Richon VM, Rifkind RA, Marks PA, Breslow R, Pavletich NP (1999) Structures of a histone deacetylase homologue bound to the TSA and SAHA inhibitors. *Nature* **401:** 188–193

Fischle W, Dequiedt F, Hendzel MJ, Guenther MG, Lazar MA, Voelter W, Verdin E (2002) Enzymatic activity associated with class II HDACs is dependent on a multiprotein complex containing HDAC3 and SMRT/N-CoR. *Mol Cell* **9:** 45–57

Gallinari P, Di Marco S, Jones P, Pallaoro M, Steinkühler C (2007) HDACs, histone deacetylation and gene transcription: from molecular biology to cancer therapeutics. *Cell Res* **17:** 195–211

Gregoretti IV, Lee YM, Goodson HV (2004) Molecular evolution of the histone deacetylase family: functional implications of phylogenetic analysis. *J Mol Biol* **338:** 17–31

Hassig CA, Tong JK, Fleischer TC, Owa T, Grable PG, Ayer DE, Schreiber SL (1998) A role for histone deacetylase activity in HDAC1-mediated transcriptional repression. *Proc Natl Acad Sci USA* **95:** 3519–3524

Holbert MA, Marmorstein R (2005) Structure and activity of enzymes that remove histone modifications. *Curr Opin Struct Biol* **15:** 673–680

Jones P *et al* (2006) A series of novel, potent, and selective histone deacetylase inhibitors. *Bioorg Med Chem Lett* **16:** 5948–5952

Kapustin GV, Fejer G, Gronlund JL, McCafferty DG, Seto E, Etzkorn FA (2003) Phosphorus-based SAHA analogues as histone deacetylase inhibitors. *Org Lett* **5:** 3053–3056

Laskowski RA (2003) Structural quality assurance. *Methods Biochem Anal* **44:** 273–303

Liu L, Scolnick DM, Trievel RC, Zhang HB, Marmorstein R, Halazonetis TD, Berger SL (1999) p53 sites acetylated *in vitro* by PCAF and p300 are acetylated *in vivo* in response to DNA damage. *Mol Cell Biol* **19:** 1202–1209

Marks PA, Miller T, Richon VM (2003) Histone deacetylases. *Curr Opin Pharmacol* **3:** 344–351

Murshudov GN, Vagin AA, Dodson EJ (1997) Refinement of macromolecular structures by the maximum-likelihood method. *Acta Crystallogr D* **53:** 240–255

Navaza J (2001) Implementation of molecular replacement in AMoRe. *Acta Crystallogr D* **57:** 1367–1372

Nielsen TK, Hildmann C, Dickmanns A, Schwienhorst A, Ficner R (2005) Crystal structure of a bacterial class 2 histone deacetylase homologue. *J Mol Biol* **354:** 107–120

Rodriquez M, Aquino M, Bruno I, De Martino G, Taddei M, Gomez-Paloma L (2006) Chemistry and biology of chromatin remodeling agents: state of art and future perspectives of HDAC inhibitors. *Curr Med Chem* **13:** 1119–1139

Roth SY, Denu JM, Allis DC (2001) Histone acetyltransferases. *Annu Rev Biochem* **70:** 81–120

Schuttelkopf AW, van Aalten DM (2004) PRODRG: a tool for high-throughput crystallography of protein–ligand complexes. *Acta Crystallogr D* **60:** 1355–1363

Sengupta N, Seto E (2004) Regulation of histone deacetylase activities. *J Cell Biochem* **93:** 57–67

Somoza JR *et al* (2004) Structural snapshots of human HDAC8 provide insights into the class I histone deacetylases. *Structure* **12:** 1325–1334

Vaghefi H, Neet KE (2004) Deacetylation of p53 after nerve growth factor treatment in PC12 cells as a post-translational modification mechanism of neurotrophin-induced tumor suppressor activation. *Oncogene* **23:** 8078–8087

Vannini A *et al* (2004) Crystal structure of a eukaryotic zinc-dependent histone deacetylase, human HDAC8, complexed with a hydroxamic acid inhibitor. *Proc Natl Acad Sci USA* **101:** 15064–15069

Vanommeslaeghe K, Van Alsenoy C, De Proft F, Martins JC, Tourwe D, Geerlings P (2003) *Ab initio* study of the binding of trichostatin A (TSA) in the active site of histone deacetylase like protein (HDLP). *Org Biomol Chem* **1:** 2951–2957

Vanommeslaeghe K, De Proft F, Loverix S, Tourwe D, Geerlings P (2005) Theoretical study revealing the functioning of a novel combination of catalytic motifs in histone deacetylase. *Bioorg Med Chem* **13:** 3987–3992

Yang XJ, Seto E (2003) Collaborative spirit of histone deacetylases in regulating chromatin structure and gene expression. *Curr Opin Genet Dev* **13:** 143–153